Spatial and temporal characteristics of the fish lateral line detection

Curcic-Blake, Branislava

Chapter 2

Experimental setup

2.1 Introduction

The displacement and velocity measurements, reported in this thesis, were performed with a Laser Interferometer Microscope (LIM). This chapter describes the LIM setup and details of its function. The setup was constructed in order to enable the detection of very small displacements (in the nm range) and the corresponding velocities of lateral line cupulae and micro-stimulus equipment in both the horizontal and vertical directions.

The technique of laser interferometry is based on two laser beams that interfere. At least one beam is reflected from the surface of the investigated object. In principle, the intensity of the light that interfered is measured, and information on either the distance or dynamics of the object is extracted. The interferometer that will be described here is of the heterodyne type, which means that the two interfering beams have different frequencies. This principle enables the measurement of displacements smaller than the wavelength of the laser light used. An advantage of this technique is that the absolute displacement or velocity can be measured, independent of the reflectance of the surface of the object. In the case of vibratory motion, simultaneously information about the phase and amplitude of the object displacement was obtained.

2.2 Laser Interferometer Microscope

The LIM setup is placed on a vibration isolated table, as shown in the photograph in Figure 2.1. The path of the light will be described in detail below. In the LIM, two plane waves reflected by the object interfere. The two beams interfere at the entrance of the photomultiplier. The intensity of the light is measured and information on the velocities and displacements is extracted from the Doppler modulation

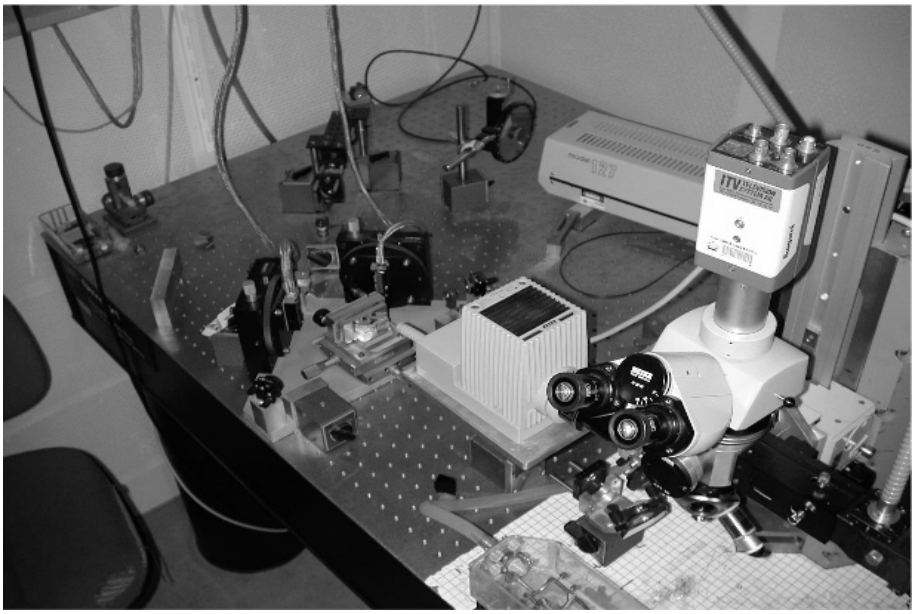

Figure 2.1: Table with LIM

of the interfered light.

We have used the LIM in two operational modes: the so-called differential and referential modes. In the differential mode, displacements and velocities of the object in the horizontal plane orthogonal to the optical axis of the microscope are measured. In the referential mode, the motion along the optical axis (vertical) of the object is measured. Only one beam is reflected from the surface of the object in this mode, and this beam interferes with the other beam at the photomultiplier.

2.2.1 Description of LIM

Schematic representations of different parts of the laser interferometer microscope are shown in Figures 2.2, 2.3 and 2.4. Figure 2.2 represents the first paths of the LIM that the laser beam follows before entering the microscope as seen from above. Figures 2.3 and 2.4 show subsequent paths of the laser beam (side view) in the two working modes of the LIM. The laser beam source was a Helium-Neon laser (Spectra Physics, model 124B), from which the Gaussian TEM_{00} mode was directed through an optical attenuator (ATT) to mirror M0, and then through lenses L1 and L2 and a $\lambda/2$ wave plate to the beam splitter BS0. The $\lambda/2$ plate was used to rotate the plane of linear polarisation at 45° to both the s and p direction, so that both reflected and transmitted beams on BS0 had equal intensity but orthogonal planes of

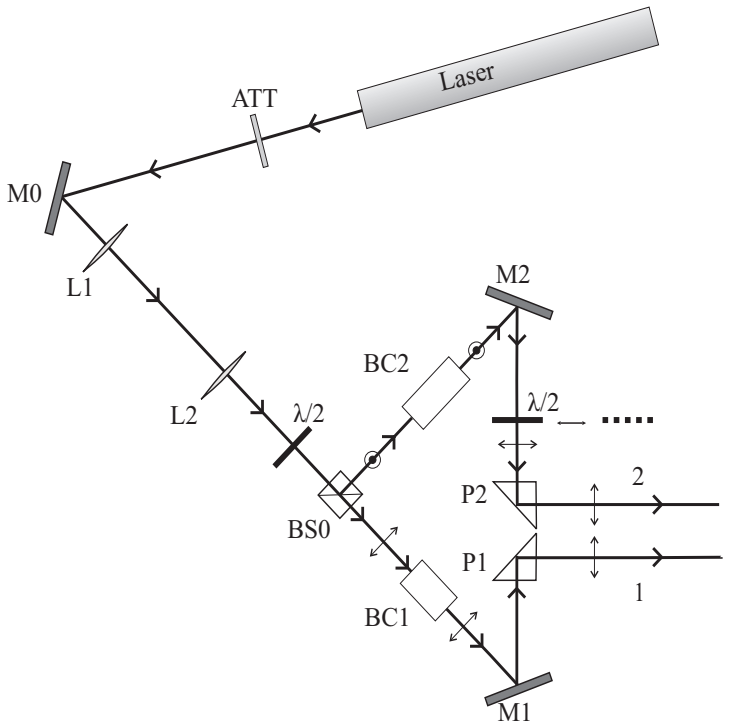

Figure 2.2: The initial part of the laser interferometer: from laser up to the entrance of two beams in the microscope. For explanation, see text

polarisation as schematically indicated by a double-headed arrow, or by concentric circles. The degree of light attenuation was tuned in each experiment according to the reflectance of the surface of the measured object, such that the signal to noise ratio of the photomultiplier was optimised without saturating the photomultiplier. The lenses L1 and L2 were inserted, forming together a telescope, to ensure that the intensity profile of the laser beams interfering at the object surface corresponded to the beam waist w_0, thus ensuring that the interference of two plane EM waves took place in the measurement volume.

The beams, split by BS0, were directed to the Bragg-cells BC1 and BC2. BC1 was driven with a frequency $f_{\mathrm{B1}} = 40$ MHz, and cell BC2 with a frequency $f_{\mathrm{B2}} = 40.4$ MHz. The outgoing beams had optical frequencies of $f_i = f_0 + f_{\mathrm{B}i}$ (i denotes the beam exiting BCi, $i = 1, 2$). The first-order diffracted beams were selected from both Bragg-cells and directed to mirrors M1 and M2.

Differential mode

The beam with the vertical plane of polarisation was passed further through a $\lambda/2$ wave plate. This rotated its polarisation back to the horizontal plane such that the two beams continued with parallel polarisations. The beams were reflected from prisms P1 and P2 towards mirror M3 (Figure 2.3). From mirror M3 both beams were redirected upward to the polarizing beam splitter BS1, which reflected both beams in the horizontal direction, since both beams were plane polarised in the horizontal plane (s - polarisation).

In order to ensure that the two beam paths were parallel and aligned well, mirrors M1, M2 and M3, prisms P1 and P2, and beam splitter BS1 were all adjustable over small angles. The beams passed next through a lens, a half mirror HM1, and were then focused on the object (Ob) by the microscope objective lens OL (Zeiss, 40x, WI, 0.8). The interference pattern of the beams had a fringe-like intensity distribution, forming a set of light and dark lines in the focal plane of the object that appeared to the observer to travel in the direction of the beam intersection plane due to the difference in frequency. The distribution of light and dark lines changed with constant velocity, which was correlated with the difference in frequency of the beams (see section 2.3.1). If the fringe pattern was imaged on a reflecting object, the travelling interference pattern was reflected and detected by the photomultiplier (PM). The displacement of the object modulated this pattern (see Equation 2.2).

As shown in Figure 2.3, the reflected light passed through a set of lenses and half mirrors (HM1 and HM2). The main part of the reflected beams was directed towards the photomultiplier through the pinhole PH. A small fraction of the reflected beams travelled to the eye-pieces (ep). The position of pinhole PH could be adjusted while being monitored through the eyepieces (ep) together with the object by back-illumination with light source (S2). This light source produced an image of the pinhole, via HM2 and BS2 on mirror M5, which was placed in a plane that was conjugate with the object plane. Seen through the eyepieces (via reflection by HM2), the pinhole had therefore equal dimensions and position as the directly imaged pinhole (via reflection by HM2), so that its position could be conveniently adjusted. The object of interest was visualised using polarised light from the halogen source S1.

Referential mode

Figures 2.2 and 2.4 illustrate the referential mode. This mode was obtained by removing the $\lambda/2$ wave plate between M2 and P2 (Figure 2.2). Then, the beam reflected from P2 (reference beam) was polarised vertically (p-polarization) and passed through beam splitter BS1 (Figure 2.4), followed by BS2 and a correcting lens. The quarter wave plate ($\lambda/4$) then changed the light from vertically plane-polarised to right-handed circularly-polarised. On reflection from mirror M5, the polarisation of the beam became left-handed, and on passing through the quarter plate for a second time it became s-polarized, so that the beam was then reflected

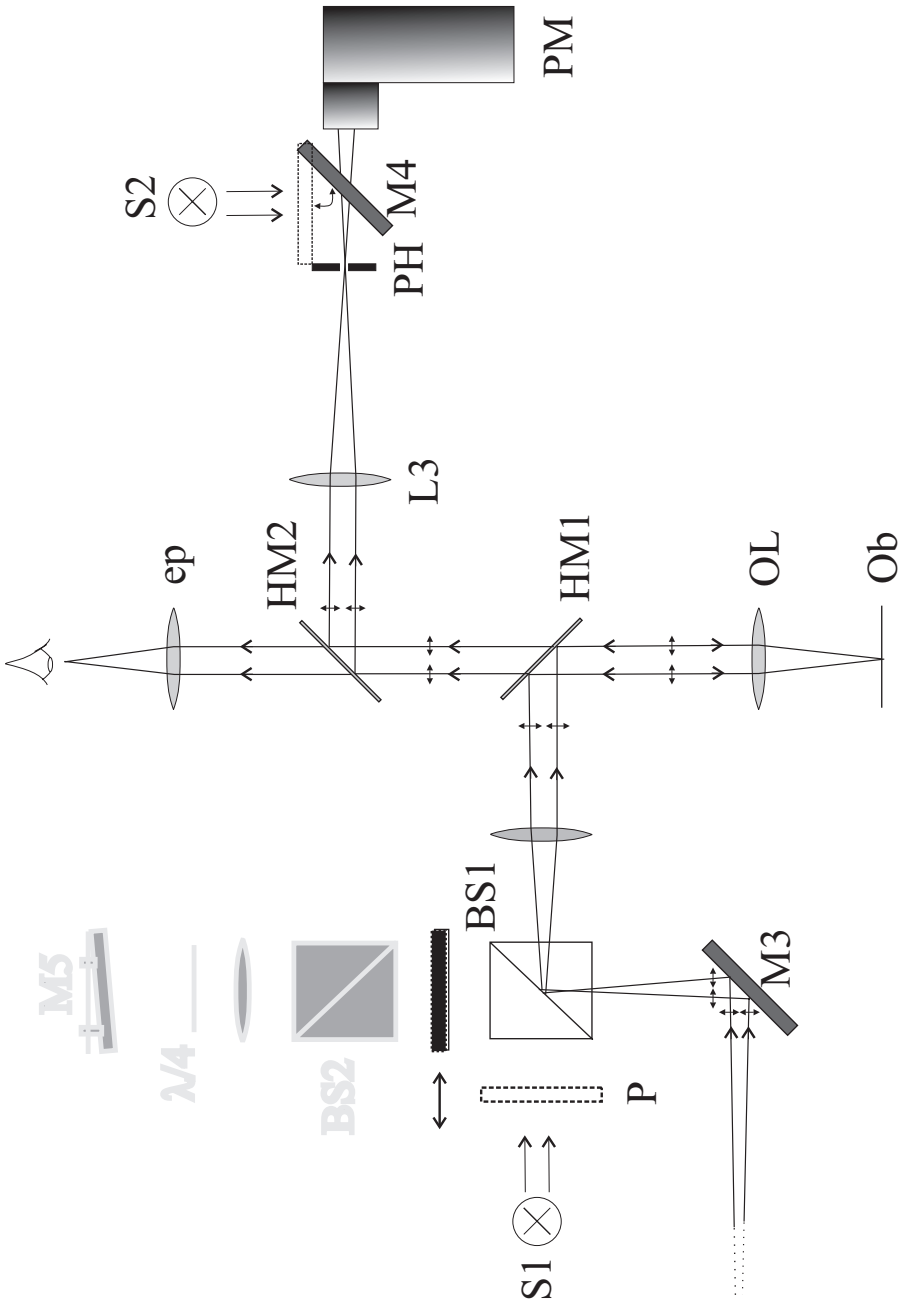

Figure 2.3: The final part of the laser interferometer for the differential mode

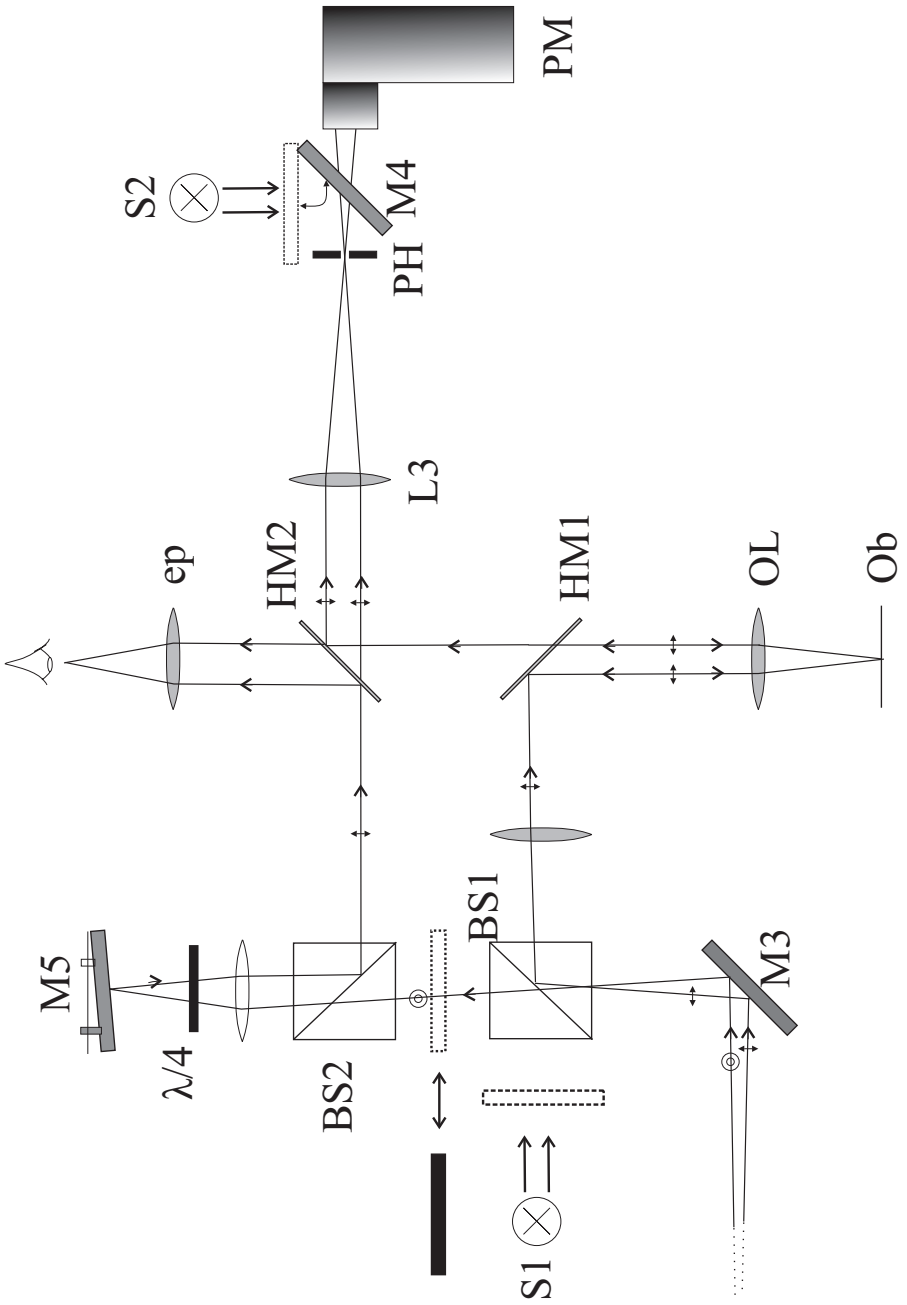

Figure 2.4: The final part of the laser interferometer for the referential mode. For explanation, see text

from BS2, via HM2, towards the photomultiplier.

The other laser beam (object beam), originating from BC1 (Figure 2.2), followed the same path as the beams in the differential mode, so that only this beam was reflected from the observed object. Since the two beams had the same plane of polarisation on arrival at the photomultiplier, they interfered. In the referential mode pinhole PH had a similar role, as in the differential mode, in imaging only the two laser beams onto the photomultiplier and rejecting unwanted and stray light. Adjusting BS2 enabled the reference beam to be focused through the pinhole. For the referential mode to work, both beams had to be parallel and superimposed. This could be achieved by adjusting M5, so that, while the reference beam remained focussed through the pinhole, its direction could be changed and aligned in parallel with the object beam to ensure full interference at the photomultiplier.

2.3 Interference of electromagnetic waves

2.3.1 Differential mode

Let us consider two plane waves (Figure 2.5), u_1 and u_2, with different optical frequencies ω_1 and ω_2:

$$u_1(x) = u_{01}e^{j(\omega_1 t+\mathbf{k_1}\cdot\mathbf{x}+\varphi_1)}$$

$$u_2(x) = u_{02}e^{j(\omega_2 t+\mathbf{k_2}\cdot\mathbf{x}+\varphi_2)}$$

Here u_{01} and u_{02} are the amplitudes of waves 1 and 2, respectively, φ_1 and φ_2 are their initial phases, and $\boldsymbol{k}_1$ and $\boldsymbol{k}_2$ are the wave vectors. If these two waves are superimposed, the outcome is the sum of the two waves, $u_{\text{tot}} = u_1 + u_2$, with an intensity:

$$I = u_{\text{tot}} \cdot u^*_{\text{tot}}$$

that can be expressed as:

$$I = u_{01}^2 + u_{02}^2 + 2u_{01}u_{02}\cos\left[(\omega_1 - \omega_2)t + (\mathbf{k}_1 - \mathbf{k}_2)\cdot\mathbf{x} + (\varphi_1 - \varphi_2)\right] \tag{2.1}$$

Consider the geometry as depicted in Fig. 2.5. The direction of vibration of the object was at an angle β with respect to the plane formed by the two beams (see Figure 2.5). Let x be the horizontal axis and z the vertical axis, then the wave vectors then have components in both the x and z directions and can be written as follows:

$$\mathbf{k}_1 = k_{1x}\mathbf{e}_x + k_{1z}\mathbf{e}_z = k_1\sin\alpha\mathbf{e}_x - k_1\cos\alpha\mathbf{e}_z$$

and

$$\mathbf{k}_2 = k_{2x}\mathbf{e}_x + k_{2z}\mathbf{e}_z = -k_2\sin\alpha\mathbf{e}_x - k_2\cos\alpha\mathbf{e}_z$$

so that

$$(\mathbf{k}_1 - \mathbf{k}_2)\cdot\mathbf{x} = (k_1\sin\alpha + k_2\sin\alpha)x$$

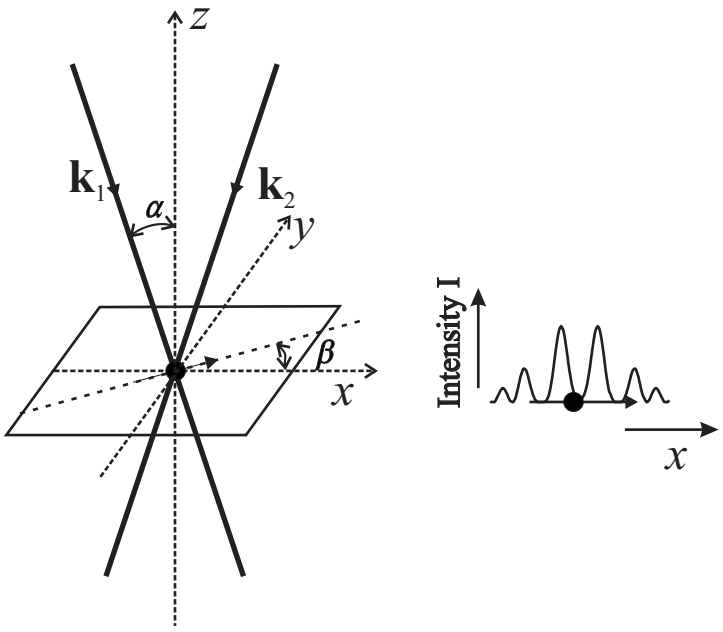

Figure 2.5: Interference of two laser beams on the vibrating object

where $\mathbf{e}_x$ and $\mathbf{e}_y$ are the unit vectors along the x- and y-axes. In the symmetrical case, where the two waves have the same amplitude and approximately the same absolute wave number ($u_{01}= u_{02}= u_0$; $|\mathbf{k}_1| \cong |\mathbf{k}_2| = k$), equation 2.1 is simplified to:

$$I = 2u_0^2 \{1 + \cos[(\omega_1 - \omega_2)t + 2kx\sin\alpha + (\varphi_1 - \varphi_2)]\}$$

With $\omega = 2\pi f$, and taking into account that $k = 2\pi/\lambda$, we obtain

$$I = 2u_0^2 \left\{1 + \cos[2\pi(f_1 - f_2)t + \frac{4\pi x\sin\alpha}{\lambda} + (\varphi_1 - \varphi_2)]\right\} \tag{2.2}$$

This expression represents an interference pattern along the x-axis (see Figure 2.5) with effective wavelength λ_{fr} (the distance between two successive peaks in the interference pattern), which can be expressed as (cf. Drain 1980):

$$\lambda_{\text{fr}} = \frac{\lambda}{2\sin\alpha}$$

All experiments were performed in water, with an index of refraction $n = 1.33$. Also, the direction of vibration of the object which is moving as $r(t)$ with an angle

β with respect to the x-axis (see Figure 2.5), along which its projected position is thus $x(t) = r(t)\cos\beta$. Combining these two conditions leads to an optical distance $x(t) = n \cdot r(t)\cos\beta$. Equation 2.2 can then be rewritten as:

$$I = 2u_0^2\{1 + \cos\phi(t)\} \tag{2.3a}$$

with

$$\phi(t) = 2\pi(f_1 - f_2)t + \frac{4\pi n \sin\alpha\cos\beta}{\lambda} r(t) + (\varphi_1 - \varphi_2) \tag{2.3b}$$

Equations 2.3a and b show that the photomultiplier signal, which is proportional to the intensity I, consists of a carrier frequency (has a phase increasing monotonically with time) equal to $(f_1 - f_2)$ of which the phase has a constant component $(\varphi_1 - \varphi_2)$ and a varying component, $\frac{4\pi n \sin\alpha\cos\beta}{\lambda} r(t)$, which is proportional to the displacement of the object. This last property lies at the basis of the two demodulation schemes used to determine either the speed (frequency-demodulation) or the displacement (phase-demodulation) of the object.

2.4 Data recording and demodulation of the signal

The photomultiplier signal was band-pass-filtered and passed to a demodulator. The output signal of the demodulator was amplified, filtered and stored on a PC via a 16-bit AD converter (Ariel, DSP-16). A modified Polytec OVF 3000 unit, with two calibrated output modes representing: 1. the velocity (analog frequency demodulator) and 2. the displacement (digital phase demodulator), was used in the submicrometer measurements described in this thesis.

1. The output of the Polytec OFV-3000 frequency demodulator is a voltage, which is proportional to the velocity of the measured object. This demodulator is based on a phase-locked loop circuit and detects the changes in instantaneous frequency of a signal. This, in the differential mode, effectively determines the time derivative of the phase $\phi/2\pi$,

$$\frac{1}{2\pi}\frac{\mathrm{d}\phi(t)}{\mathrm{d}t} = (f_1 - f_2) - \frac{2n\sin\alpha\cos\beta}{\lambda}\frac{\mathrm{d}r(t)}{\mathrm{d}t} \tag{2.4}$$

   of which the last (high-pass) term is put out as a voltage with a sensitivity R_v, which in most of the experiments was $R_\mathrm{v} = 1$ V/(3164.6 Hz) (bandwidth 35 kHz).

2. The output of the Polytec OFV-3000 phase demodulator is a voltage, which is proportional to the displacement of the measured object. The digital phase demodulator is based on a fringe counting scheme with a selectable sub-fringe resolution, which was usually set to either 8 or 32 nm. The modulator subtracts the monotonically growing phase component of Eq. 2.3b, which is

related to the frequency difference $(f_1 - f_2)$ and puts out a voltage proportional to the remaining displacement dependent component, $\frac{2n \sin \alpha \cos \beta}{\lambda} r(t)$, with a sensitivity R_d = 1 V/ (39.7 rad) or 1 V/(158.7 rad) (bandwidth 50 kHz).

In both cases, λ is the wavelength of the laser beam (λ = 632.8 nm), α is the half angle between the two interfering beams, and $n = 1.33$ is the refractive index of water. The numerical aperture of the objective lens used (Zeiss, 40 WI, N.A. = 0.8) restricts α to about 37°, while β, the angle between the object's motion and the plane of the laser beams (Fig. 2.5), was usually about 30°. Using the above equations and settings we are able to obtain the velocity or displacement in the differential mode. In the referential mode only one beam was directed to the object. We therefore replaced the factor 2 sin α by 1 + cos α.

2.5 Sensitivity of the measurements

The accuracy of heterodyne laser interferometric measurements is in principle limited by genuine photon noise, photomultiplier noise, and broadening of the Doppler frequency signal. The latter effect can be caused by, for example, improper focusing of the beam crossing; a distance of tens of micrometers between the beam crossing point and the beam waists could result in an error of $\sim 20\%$ (Hanson 1973). In our experiments this error is minimised by the use of the telescope system produced by lenses L1 and L2 (e.g. van Netten 1988). The signal to photon noise ratio for a similar setup was calculated by van Netten (1988) for the case of the differential mode and was estimated to be approximately of the order of 10 under similar reflectivity properties (< 0.002) as used in the present studies.

The velocity or displacement accuracy depends on the working range of the demodulator and the bandwidth used, so that it increases with the square root of the number of measurements used to obtain an average. In our experiments the displacement was usually measured with an accuracy estimated to be as small as 1.5 nm. The accuracy of the velocity measurements was estimated to be approximately 0.6 μm/s.

2.6 Summary and conclusions

The LIM setup can be used in two modes, differential and referential, to measure sub-micrometer vibratory displacements up to the kHz range and related velocities, both at right angles (horizontal) and parallel (vertical) to the optical axis of the objective lens respectively. It is suitable for measuring displacements of biological objects with low reflectance (tenths of a percent or lower). Displacements of transparent lateral line cupulae as small as 1.5 nm can be measured with this technique. The additional noise caused by oscillating mechanical mounts and supports of the

optical devices in the differential mode is cancelled out by passing both laser beams through closely mounted optical devices, so that the optical path difference that is effectively detected is minimally affected. The accuracy of measurements in both modes is fundamentally limited by photon noise, and therefore can be improved by longer measurements and subsequent averaging (or equivalently by reducing the bandwidth). The reference beam (in referential mode) can be set at a higher intensity in comparison to the beam scattered from the object, which, in principle may enhance the accuracy of measurement in this mode and thus has an advantage with respect to the differential mode (cf. Drain 1980).